Phase Structure of Poly(dimethylsiloxane−urea−urethane)-Segmented Copolymers as Observed by Solid-State Nuclear Magnetic Resonance Spectra

Gyunggoo Cho,[†] Almeria Natansohn,*[,†] Tai Ho,[‡] and Kenneth J. Wynne[§]

Department of Chemistry, Queen's University, Kingston, Ontario K7L 3N6, Canada, Department of Chemistry, George Mason University, Fairfax, Virginia 220303-4444, Physical Sciences S&T Division-331, Office of Naval Research, Arlington, Virginia 22217-5660, and Naval Research Laboratory, Materials Chemistry Branch 6120, Washington, D.C., 20375-5320

Received June 5, 1995; Revised Manuscript Received January 2, 1996[⊗]

ABSTRACT: Three segmented copolymers having as hard segments poly(urethane−urea)s based on isophorone diisocyanate (IP) and 1,4-benzenedimethanol (B) and having as soft segments poly(dimethylsiloxane)s (PDMS) of three different molecular weights are analyzed by CP-MAS ^{13}C-NMR. Comparison of cross-polarized and non-cross-polarized spectra, together with proton relaxation measurements, establishes the presence of separated phases and differences in their mobility. The $T_{1\rho}$(H)'s and static ^{1}H-NMR half-height line widths of PDMS*y*K−IP−B_2 (y = 2.4, 10, and 27; refers to the PDMS molecular weight) give information about the motion as a function of the molecular weight of PDMS. A dipolar filter sequence is employed to estimate the size of the dispersed hard phases, which appears to be of about 5 nm for all samples. The overall (soft and hard) domain sizes increase with the increase of silicone molecular weights, as expected.

Introduction

As part of research into surfaces of minimal adhesion, poly(siloxane−urethane−urea)s have been synthesized and characterized.[1] An ESCA study of the polymer surface showed that there is a considerable enrichment of the siloxane soft segment at the surface and that a subsurface-enriched hard block zone exists.[2] A typical polymer containing long poly(dimethylsiloxane) segments has the following repeating structure:

$$...A[B(CB)_x]...$$

with A−C indicated in Chart 1. The samples analyzed in this paper are abbreviated PDMS*y*K−IP−B_2 and were obtained from poly(dimethylsiloxane) (PDMS) of different molecular weights (2400, y = 2.4; 10 000, y = 10; 27 000, y = 27), 5-isocyanato-1-(isocyanatomethyl)-1,3,3-trimethylcyclohexane (IP), and 1,4-benzenedimethanol (B) in a ratio of 1PDMS:3IP:2B following a procedure described previously.[1]

Probably the best technique to offer insight into the phase structure of these materials is ^{13}C high-resolution solid-state NMR. The presence of different phases in an apparently homogeneous material can be easily proven by proton relaxation time constants. It is well known that the cross-polarization procedure, which uses proton magnetization as the reservoir, reflects spin diffusion throughout the sample. If various phases are present, spin diffusion will be somewhat impeded and more than one diffusion constant will be measured for the sample. The laboratory frame and rotating frame measurements will offer insight at various domain size levels, with the rotating frame being sensitive almost to the molecular level.[4] A better method yet to look at the phase structure is based on the selective excitation of one phase followed by monitoring of spin diffusion until the magnetization reaches equilibrium. This was initially proposed by Goldman and Shen[5] and subsequently developed by a number of research groups, based on various selection procedures. Spiess et al.[6−9] proposed a dipolar filter pulse sequence which is applicable to phase-separated systems containing a rubbery component. This pulse sequence uses a series of pulses to select the rubbery component and then monitors the magnetization going back to equilibrium in the rest of the sample.

This paper presents CP-MAS ^{13}C-NMR experiments on the three PDMS*y*K−IP−B_2 (y = 2.4, 10, and 27) samples which help in identifying the phase structure, dynamics, and sizes.

Experimental Section

Proton-decoupled solid-state ^{13}C-NMR spectra were recorded at 50.29 MHz on a Bruker ASX-200 spectrometer using cross-polarization and magic angle spinning at room temperature. Solid-state ^{1}H-NMR spectra were acquired on a Bruker ASX-200 at 200 MHz. The $\pi/2$ pulse length was 3.7 μs, and the delay between pulses was 5 s. The spinning rate for all spectra was 3.00 kHz. The cross-polarization time was 0.5 ms. T_1(H) was measured with an inversion-recovery pulse sequence, while $T_{1\rho}$(H) for siloxane was obtained by using ^{1}H-NMR detection. $T_{1\rho}$(H) for the hard segment was obtained using a variable delay and maintaining a constant contact time. The dipolar filter sequence[6] had 12 $\pi/2$ pulses with 13 μs spacing between them, and typically it had to be repeated seven times to give a good selection. A schematic representation of this pulse sequence is presented in Figure 1 for the reader who is not familiar with it. Static ^{1}H-NMR spectra were acquired with no spinning after a single $\pi/2$ pulse. Solution ^{1}H-NMR spectra were recorded at 200.133 MHz on a Bruker ACF-200 spectrometer in $CDCl_3$.

Minimization of conformational energies for models was performed using the PCMOD program (Serena Software) with a MMX force field on a Silicon Graphics computer.

Results and Discussion

The ESCA results, and the synthetic procedure, suggest the presence of a phase-separated material. A ^{1}H-NMR solution spectrum of PDMS27K−IP−B_2 is

[†] Queen's University.
[‡] George Mason University.
[§] Office of Naval Research and Naval Research Laboratory.
[⊗] Abstract published in *Advance ACS Abstracts,* March 1, 1996.

0024-9297/96/2229-2563$12.00/0 © 1996 American Chemical Society

Chart 1

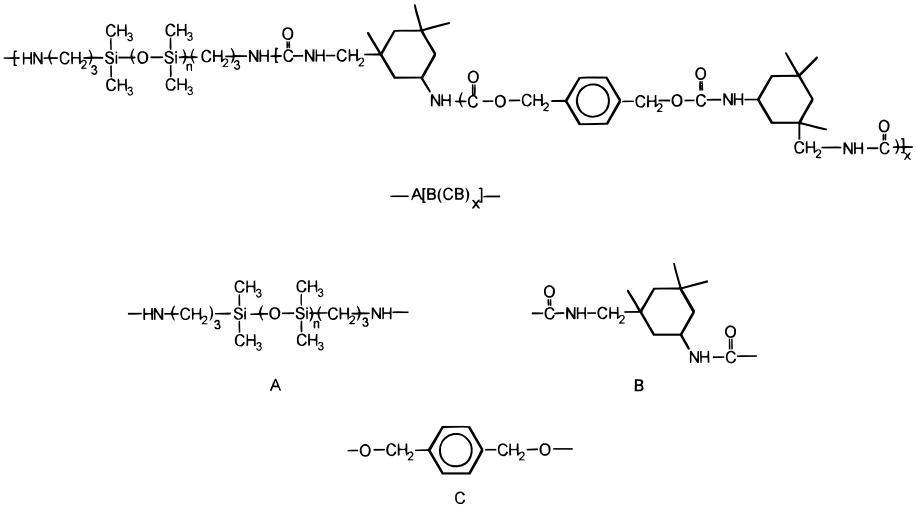

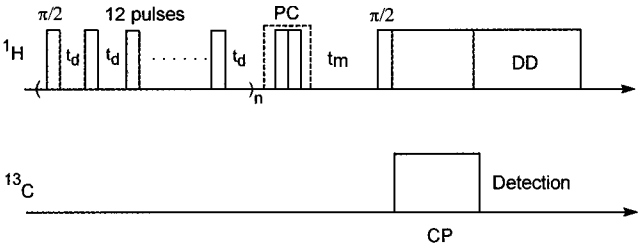

Figure 1. Dipolar filter pulse sequence. t_d was 13 μs, and n was 7. The phase cycling (PC) was used only for PDMS2.4K−IP−B_2 (see text). The $\pi/2$ pulse length was 3.7 μs, and the CP time was 0.5 ms.

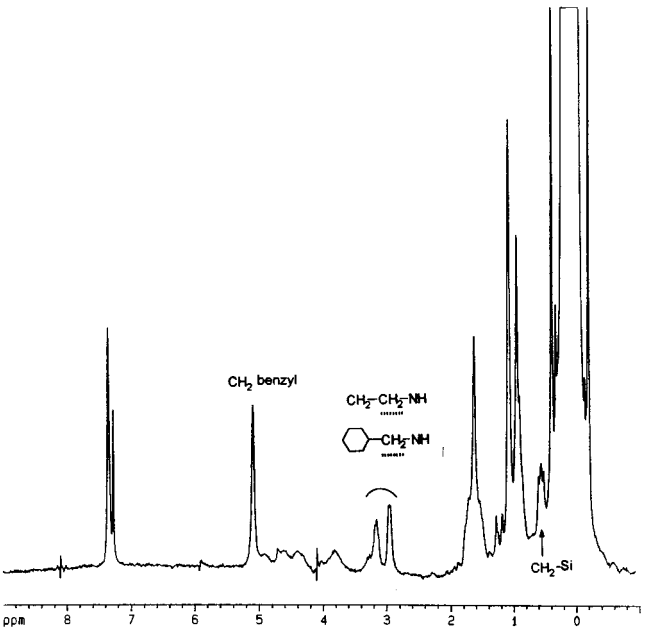

Figure 2. ^{1}H-NMR spectrum of PDMS27K−IP−B_2 dissolved in chloroform.

presented in Figure 2. The assignments are not very straightforward, but it is reasonable to assign the signal at 5.15 ppm to the benzylic methylenes (in C, Chart 1) and the triplet at 0.53 ppm to methylene groups bound directly to the silicone (in A).[1] The low-intensity broad signal between 3.5 and 4.9 ppm should include methine protons bound to NH and the NH protons themselves. There are eight such protons in the proposed formula and just four benzylic methylene protons, which is in good agreement with the signal intensities. The multiplet signal at about 3 ppm should include the methylene protons bound to the nitrogen and the cyclohexane ring (in B) and maybe the methylene protons (in A) which are directly bound to the poly(urethane−urea) segment through the nitrogen. If one uses ratios of these signals in PDMSyK−IP−B_2 (y = 2.4, 10, and 27) spectra, keeping in mind some approximate assignments and the error in the integral of the 0.53 ppm signal, due to the uncertain base line, the x value of the PDMS27K−IP−B_2 sample can be calculated to be somewhere between 1 and 2, and the x values of the other samples (PDMS2.4K−IP−B_2 and PDMS10K−IP−B_2) are about 2. Thus, the so-called "hard" segment is very short in comparison to the "soft" segment. Indeed, the thermal analysis of the PDMS27K−IP−B_2 sample by DSC only shows one first-order transition at ca. −40 °C, assigned to the melting of PDMS.[3] Dynamic mechanical analysis (DMA) for PDMS2.4K−IP−B_2 shows the glass transition of PDMS at ca. −100 °C and another apparent transition at ca. 80 °C, which is below the expected T_g of the hard segments. The DMA results seem to suggest that the PDMS2.4K−IP−B_2 sample is phase-separated, and this is the only indication for phase separation for all these samples. The question addressed here is (1) are the hard poly(urethane−urea) segments in all samples large enough to associate and form a separate phase, with a different mobility than the soft segments, or (2) do the hard poly(urethane−urea) segments simply get "diluted" in the material? ESCA results seem to indicate that the hard segments are separated; however, the thermal analysis does not identify the presence of a second, hard phase.

Phases and Mobilities. It is very easy to see in the NMR spectra that the solid samples analyzed here contain two phases of very different mobilities. A simple ^{13}C-NMR spectrum, with spinning but not cross-polarization, generates a very intense high-resolution silicone signal and nothing else. The appearance of the silicone signal is due to the very high mobility of the magnetic nuclei in the rubbery phase, and the fact that this is the only signal in the spectrum clearly indicates that the other components are much less mobile.

Spectra of the PDMSyK−IP−B_2 samples obtained with cross-polarization are shown in Figure 3. The chemical shift of the silicone peak was used as the reference at 0 ppm. The assignments of the signals have been performed with the help of dipolar dephasing experiments[10] and are given in Figure 3. The chemical

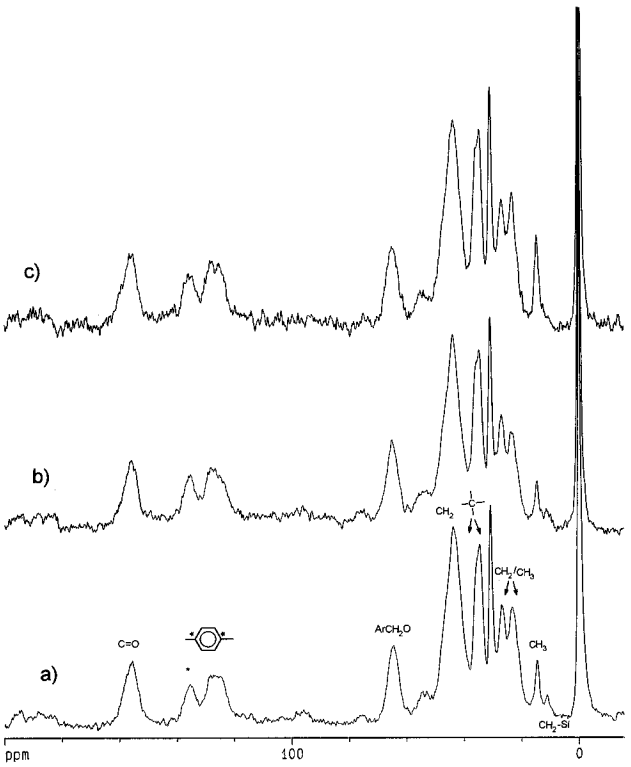

Figure 3. CP-MAS ^{13}C-NMR spectra of PDMS*y*K−IP−B_2: (a) PDMS2.4K−IP−B_2, (b) PDMS10K−IP−B_2, and (c) PDMS27K−IP−B_2.

shifts and line shapes of the peaks do not change with the increase of the molecular weight of PDMS. One indication for the different mobility of the two segments comes from the intensity of the peak at 11.1 ppm, assigned to the methylene group directly bound to Si in structure A (Chart 1). The $SiCH_2$ signal is not even visible in the sample with the highest silicone molecular weight. The explanation for this change must be related to the different mobility of the silicone segments at different segmental lengths. The methylene groups are directly bound to the soft segment, and hence their mobility will reflect the mobility of the soft segment. The efficiency of cross-polarization inversely depends on mobility, and thus one can infer that the silicone segments are less mobile when they are shorter, allowing a more efficient cross-polarization of the methylene peak.

The ratios of the number of carbons in the soft and hard phases range from about 2:1 (PDMS2.4K−IP−B_2) to 23:1 (PDMS27K−IP−B_2), and the carbons of the soft phase resonate mainly in one peak, while the carbons of the hard phase are distributed between many peaks. Therefore, a very high intensity of the silicone peak is expected, especially in PDMS27K−IP−B_2, but this is not the case. While the full intensity of the silicone peaks is not shown in the figure, this intensity is related to differences in mobility of the hard and soft phases. Since the soft phase is much more mobile than the hard phase, its cross-polarization efficiency is much lower. Figure 4 shows a plot of some signal intensities of the hard and soft phases for PDMS2.4K−IP−B_2 as a function of contact time. All signals are normalized to the highest intensity of each respective peak. Two hard phase signals (43.8 ppm, methylene carbon, and 30.8 ppm, quaternary carbon) and one signal from the soft phase (0 ppm, silicone peak) are shown as typical examples for the general behavior. With increasing contact time, the signals are expected to increase in

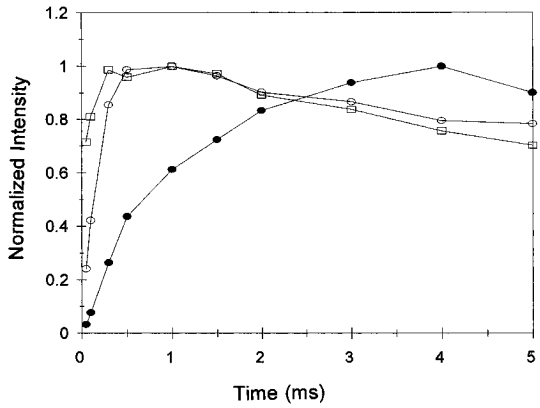

Figure 4. Plot of intensity of signals at 43.8 (□) and 30.8 (○) ppm and the PDMS signal at 0 ppm (●) as a function of contact time. All intensities are normalized to the highest intensity for each peak.

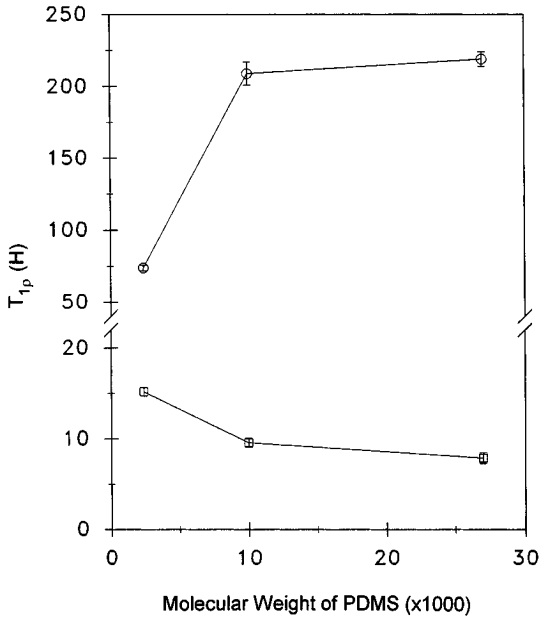

Figure 5. Plot of $T_{1\rho}$(H) of the hard (□) and soft (○) phases as a function of the molecular weight of PDMS.

intensity until the optimum transfer of magnetization is achieved, and then the signal should decay due to the rotating frame relaxation. Both hard phase signals reach their optimal cross-polarization very fast, in about 0.5 ms. The protonated signal (43.8 ppm) is faster to cross-polarize than the nonprotonated signal, which is normal behavior. The soft phase signal intensity increases up to 4 ms contact time and appears to decrease at 5 ms. From the growth pattern, its cross-polarization probably reaches an optimum at about 4 ms contact time. This poor efficiency of the cross-polarization is again due to the high mobility of this phase, and the differences in mobility for the two types of segments are obvious.

Since proton spins are abundant, spin−lattice relaxation times (T_1(H), in the laboratory frame, and $T_{1\rho}$(H), in the rotating frame) of polymers can be used to investigate the phase structure in polymers. T_1(H) measurements produce a single value for each sample, indicating magnetic homogeneity at that level within the sample. Figure 5 shows the plot of $T_{1\rho}$(H) values of the PDMS*y*K−IP−B_2 samples as a function of the molecular weight of PDMS. Each sample has two different $T_{1\rho}$(H) values, one for the soft segment and the other for the hard segment (assigned by carbon detec-

tion), which indicate phase separation. From Figure 4, as the molecular weight of PDMS increases, the $T_{1\rho}$(H) of the hard segment decreases and the $T_{1\rho}$(H) of the soft segment increases at least between 2.4 and 10 KDa. $T_{1\rho}$(H) values are mainly determined by dipolar interaction which depends on the motion of protons and on proton density. If we assume that the proton densities of the hard and soft phases are invariant with the increase of the molecular weight, the change of $T_{1\rho}$(H)'s for both phases is produced by motional changes. $T_{1\rho}$(H) has been used to investigate the frequency of motions in polymers.[11] As a function of frequency, in the kilohertz range, $T_{1\rho}$(H)'s decrease on the low-temperature side of minima and do not change on the high-temperature side of minima as the radiofrequency fields decrease. To establish on which side of the $T_{1\rho}$(H) minimum is room temperature, a measurement of $T_{1\rho}$(H)'s can be performed at different radiofrequency fields. The $T_{1\rho}$(H)'s of the hard phase PDMS*y*K−IP−B_2 decrease (15.2 to 13 ms for PDMS2.4K−IP−B_2, 9.6 to 8.5 ms for PDMS10K−IP−B_2, and 8.1 to 6.2 ms for PDMS27K−IP−B_2), and those of the soft phase do not change when the field is changed from 67.5 to 50 kHz (90° pulses of 3.7 and 5.0 μs). This means that the soft phase is on the high-temperature side of the minimum, i.e., its motion is liquid-like, which is expected, since it generates a "liquid" spectrum (without cross-polarization) in its solid state. An increase of the temperature (and of the motion) should generate a less efficient relaxation in the rotating frame, hence a higher $T_{1\rho}$(H). The hard phase is on the low-temperature side of the minimum, which means that an increase in temperature (hence motion) will increase the efficiency of relaxation and lower the $T_{1\rho}$(H).

Both these features (the $T_{1\rho}$(H) increase of the soft phase and the $T_{1\rho}$(H) decrease of the hard phase) occur when the silicone molecular weight increases, appearing to suggest an increase in mobility for both phases. Obviously, this explanation is correct only if the total surface area separating the phases is approximately constant for all samples. This is not necessarily true. Also, the $T_{1\rho}$(H) value is an average for the whole phase. A rigid dispersed phase may appear more mobile just because there are more mobile interfacial areas of contact with the continuous phase. With those caveats, one can notice a large change in $T_{1\rho}$(H) between 2.4 and 10 KDa molecular weights and little change above 10 KDa. This may indicate motional changes which are more important at lower molecular weights.

The degree of motional differences of PDMS in the PDMS*y*K−IP−B_2 samples (2.4, 10, and 27 KDa) can be also estimated by the ^{1}H-NMR line widths. The static ^{1}H-NMR half-height line widths ($\Delta\nu_{1/2}$) of the PDMS*y*K−IP−B_2 samples (2.4, 10, and 27 KDa) are 1100, 560, and 450 Hz, respectively. This confirms that the motional differences of PDMS are greater between PDMS2.4K−IP−B_2 and PDMS10K−IP−B_2 than between PDMS10K−IP−B_2 and PDMS27K−IP−B_2.

From the results of the $T_{1\rho}$(H)'s, the ^{1}H-NMR line widths, and the cross-polarization efficiency of the methylenes bound to Si, we conclude that the presence of a poly(urea−urethane) segment next to a PDMS segment appears to affect the motion of the soft segment. With shorter silicone segments (2.4 KDa), the hard phase retards the motion of PDMS, but when the molecular weight of the siloxane segment exceeds 10 KDa, the effect of the hard phase in retarding the PDMS motion is lessened. There are not enough data to conclude if this change in motion is intrinsic or if it appears from a significant change in the volume ratio interface/bulk. At lower molecular weights, the amount of interface (experiencing restricted motion) may be significant enough to affect the apparent overall motion of the soft phase.

Table 1. Average Spin Traveling Distances in the Hard Segment of PDMS*y*K−IP−B_2 during $T_{1\rho}$(H)'s and T_1(H)'s

	distance (nm)	
	$T_{1\rho}$(H)	T_1(H)
PDMS2.4K−IP−B_2	3.5	27.4
PDMS10K−IP−B_2	2.8	30.2
PDMS27K−IP−B_2	2.6	28.8

Phase Size Estimates. The T_1(H)'s of the PDMS*y*K−IP−B_2 samples (2.4, 10, and 27 KDa) are 910, 1100, and 1000 ms respectively. There is a single T_1(H) for all signals in the spectrum. If ^{1}H-NMR magnetization reaches equilibrium during the relaxation time, even polymers having more than one phase show the same relaxation time. Therefore, the equilibrium time of ^{1}H-NMR magnetization for each PDMS*y*K−IP−B_2 sample must be between the $T_{1\rho}$(H) and T_1(H) values. The spin equilibrium time depends on the domain size and the spin diffusion coefficients of different phases. The minimum size level that can be obtained from the spin−lattice relaxation times can be estimated by the following equation:[12]

$$\langle\delta^2\rangle = 4Dt/3 \qquad (1)$$

where δ is the spin traveling distance in time t (which here has to be equated with the spin−lattice relaxation time) and D is the spin diffusion coefficient. To estimate the minimum phase size, one needs the spin diffusion coefficient of the poly(urethane−urea), which is not available. The literature is very scarce in studies reporting spin diffusion coefficients for various materials, although some recent studies have begun to report such data. As an approximation, the spin diffusion coefficient of alkane (6.2×10^{-16} m^2/s)[13] can be used here as a substitute for the unknown poly(urea−urethane) diffusion coefficient. Table 1 shows the average spin traveling distances in the hard segment of PDMS*y*K−IP−B_2 obtained from the spin−lattice relaxation times of the hard segments. The actual hard segment phase size (dispersed phase size) should be greater than the average spin traveling distance during $T_{1\rho}$(H) and smaller than it during T_1(H) because two relaxations are seen at the rotating frame level and only one at the laboratory level. For example, for PDMS2.4K−IP−B_2, the dispersed phase size should be between 3.5 and 27.4 nm.

Magnetization Transfer. In order to find out the size of hard segment phase, a dipolar filter pulse sequence has to be employed for these materials.[6] Normally, prior to applying a dipolar filter pulse sequence, one should verify the different mobility of the two phases using a wide-line separation two-dimensional spectrum,[14,15] but in this case this is not necessary: The two phases have been shown to differ significantly in motion. The multiple pulse in the proton domain (shown in Figure 1) will average relatively small dipolar couplings of the protons, typically those belonging to rubbery (very mobile) phases. The spacing between pulses allows large dipolar couplings (those in more rigid phases) not to be effectively averaged; the magnetization of the corresponding protons then relaxes. The result of this repeated multiple pulse is that

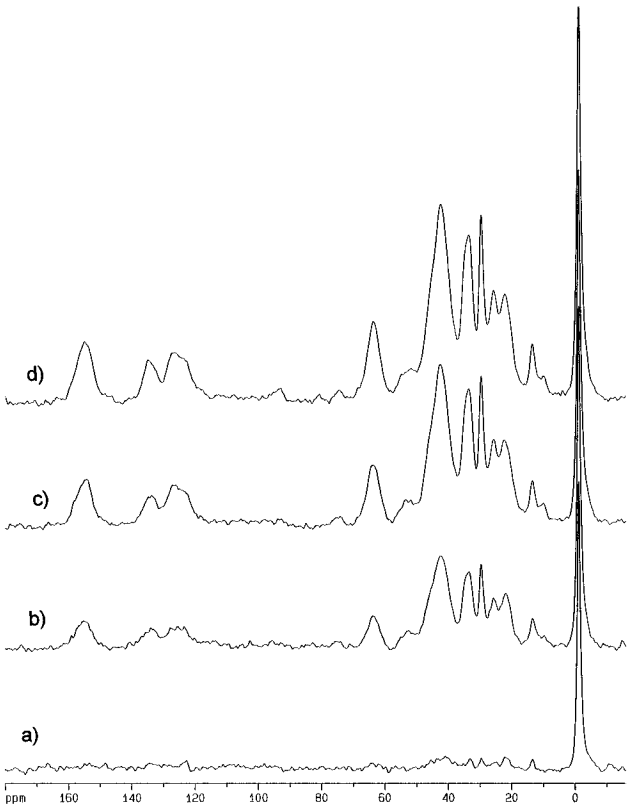

Figure 6. CP-MAS ^{13}C-NMR spectra of PDMS2.4K−IP−B_2 obtained with the dipolar filter pulse sequence at various mixing times: (a) 50 μs, (b) 5 ms, (c) 30 ms, and (d) 100 ms. The number of scans was 2048.

the only remaining magnetization in the spectrum belongs to mobile domains. The corresponding spectrum (with the minimum possible mixing time (t_m) of 50 μs) is shown in Figure 6a for PDMS2.4K−IP−B_2. At 50 μs mixing time, the silicone peak is selected and signals from the hard phase are in the noise. Increasing the delay between selection and detection (mixing time), the magnetization is allowed to equilibrate over the whole sample, and the signals for the hard phase start being detected. The magnetization of the hard phase for this sample grows quickly with increasing the mixing time and reaches equilibrium in about 150 ms. One should note that the magnetization of the hard phase grows by both spin diffusion and T_1 during the mixing time. At long mixing times (compared to T_1), the T_1 contribution to magnetization makes it too difficult to find an equilibrium time. The phase alternation (π pulse between the dipolar filter and the mixing time at every other scan appearing as PC in Figure 1) partially cancels the magnetization due to T_1, and the evolution of the magnetization is mostly due to spin diffusion. The real magnetization for spin diffusion measurements is the experimental magnetization multiplied by the correction factor $\exp(t_m/T_1)$.[8] PDMS*y*K−IP−B_2 samples equilibrate fast compared with—say—a triblock copolymer with a dispersed phase size of about 16 nm, which requires some 300 ms to reequilibrate.[16] The magnetization of the hard phase for PDMS10K−IP−B_2 and PDMS27K−IP−B_2 reaches equilibrium much faster, within 50 ms. Since the equilibrium times of magnetization of the PDMS10K−IP−B_2 and PDMS27K−IP−B_2 samples due to spin diffusion are about 20 times less than T_1 relaxation times, dipolar filter pulse sequences without the phase alternation were used for these samples.

The magnetization growth following the dipolar filter sequence can be used to estimate domain sizes. Plots of intensities vs the square root of mixing times have been used either to measure the spin diffusion coefficients from known domain sizes or to determine the domain sizes from known spin diffusion coefficients through simulation.[8,9] The model used to obtain these parameters assumes that the two phases exchanging magnetization are interchangeable and that it makes no difference which of the phases is the source of magnetization. If spin diffusion coefficients within a hard and a soft phase are known, a dispersed domain size can be calculated using the plot of intensity vs the square root of mixing time and eq 2:[9]

$$d_{dis} = \left(\frac{\rho_{HA}\phi_A + \rho_{HB}\phi_B}{\phi_A\phi_B}\right) \times \frac{4\phi_{dis}\epsilon\sqrt{D_A D_B}}{\sqrt{\pi}(\sqrt{D_A}\rho_{HA} + \sqrt{D_B}\rho_{HB})}\sqrt{t_m^*} \quad (2)$$

where ρ_H is the proton density in each phase and Φ is the volume fraction of each phase. Φ_{dis} is the volume fraction of the dispersed phase, which in this case is the poly(urethane−urea) segment. From the estimated densities of the two phases and the number of protons in each, these parameters can easily be calculated. The spin diffusion coefficients of either phase (D_A and D_B) are unknown and have to be approximated. It is expected that the change in motion would affect the spin diffusion coefficients of PDMS segments. Spiess and coworkers have studied in comparison the spin diffusion coefficients and the ^{1}H-NMR half-height line widths of rubbery phases using polybutadiene at different temperatures.[8] As the ^{1}H-NMR half-height line width increases from ca. 200 to ca. 600 Hz, the spin diffusion coefficient of polybutadiene increases only slightly from 0.5×10^{-16} to 0.6×10^{-16} m^2/s[8]. In our case, the real spin diffusion coefficient of the soft phase is not known, but the difference of the ^{1}H-NMR half-height line width between PDMS2.4K−IP−B_2 and PDMS27K−IP−B_2 is not large. Therefore, for poly(dimethylsiloxane), it would be a good approximation to use the spin diffusion coefficient measured for polybutadiene (0.5×10^{-16} m^2/s), as Spiess did,[8] while for the hard segments, the alkane spin diffusion coefficient can be used, as was done for the relaxation parameters. ϵ is a coefficient indicating the dimensionality of the system, thus making this equation valid for any kind of sample morphology. The calculated weight fractions of the hard phase for PDMS*y*K−IP−B_2 (y = 2.4, 10, and 27) are 0.31, 0.10, and 0.03, respectively. The dimensionality of immiscible segmented copolymers depends on the volume fraction of the components. Usually, copolymers having equal volume fractions show simple one-dimensional phase structures.[15] As the volume fraction of one component increases, the copolymers show higher dimensional phase structures.[17] Since the density of poly(urethane−urea) (1.08 g/cm^3) is close to that of PDMS (0.95−0.98 g/cm^3), the weight fraction can be approximated by the volume fraction. Hence, the PDMS2.4K−IP−B_2 sample is assumed to be two-dimensional, and the other two samples should have three-dimensional phase structures. The square root of t_m* is read from the plot as shown in Figure 7, where magnetization growth in PDMS2.4K−IP−B_2 is illustrated, by extrapolating the linear growth of the signal to saturation level. The dispersed domain size can be

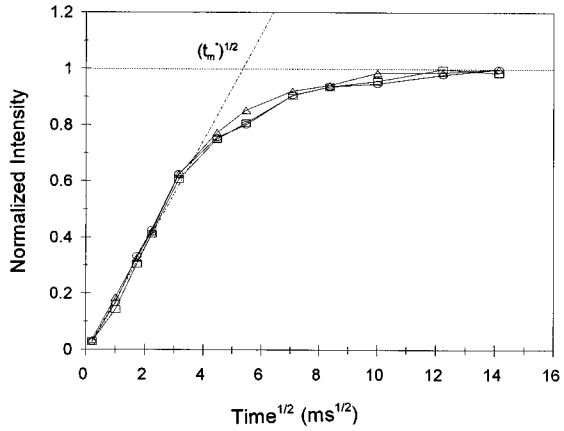

Figure 7. Magnetization growth of the peaks of the PDMS2.4K−IP−B_2 at 43.8 (□), 34.6 (△), and 30.8 (○) ppm as a function of the square root of mixing time. All intensities are corrected by $\exp(t_m/T_1)$ and normalized to the highest intensity.

calculated with eq 2, and the overall domain size can then be calculated using eq 3:

$$d = \frac{d_{dis}}{\sqrt[\epsilon]{\phi_{dis}}} \tag{3}$$

The results of the phase size calculations are shown in Table 2. The sizes of the dispersed phase of PDMS2.4K−IP−B_2 and PDMS10K−IP−B_2 are almost the same and a bit smaller for PDMS27K−IP−B2. This may be due to a slightly higher experimental error in measuring the intensities of PDMS27K−IP−B2 signals because the hard phase signals in this sample are smaller than in the other samples. Within the range allowed by all the approximations made to obtain d_{dis}, it is fair to say that the size of the hard phase is about the same for all samples. However, the shape of the hard phase is assumed to be spherical for 27 and 10 KDa ($\epsilon = 3$) and cylindrical for 2.4 KDa ($\epsilon = 2$). As the molecular weight of PDMS increases, an increase in the overall size is expected. This appears to be true in the last column of Table 2, but the change in the overall size is smaller when the threshold from cylindrical to spherical geometry is crossed. The overall size (presumably the average distance between the centers of the hard phase spheres) increases more between 10 and 27 KDa.

When the dimensionality of the dispersed (urethane−urea) phase is 3, i.e., in the cases of PDMS10K−IP−B_2 and PDMS27K−IP−B_2, the dispersed phase consists of spheres and the two hard segments end capping the same segment are not likely to be in the same sphere. A sphere of diameter 5.5 nm may contain a minimum of eight hard segments (calculated on the basis of longest end-to-end distance and excluded volume) and a maximum of 60 (calculated on the basis of hard segment density). Since there is no clear melting point observed for the hard segment block, the block is unlikely to consist of regularly packed segments and the number of segments per block should be closer to the lower extreme. Therefore, the average distance between the centers of two neighboring spheres minus the sphere diameter, $d - d_{dis}$, should be very close to the root-mean-square end-to-end distance, $\langle r^2\rangle^{1/2}$, of the soft segments. We calculated the $\langle r^2\rangle^{1/2}$ for PDMS (MW = 10 and 27 KDa) using the formula derived by Flory,[18] and the values were 73 and 120, respectively. These values are

Table 2. Square Root of t_m* and Domain Sizes of the PDMS*y*K−IP−B_2 Samples[a]

	$(t_m^*)^{1/2}$ (ms$^{1/2}$)	d_{dis} (nm)	d (nm)
PDMS2.4K−IP−B_2	5.4	5.6	10.1
PDMS10K−IP−B_2	4.7	5.5	11.8
PDMS27K−IP−B_2	4.6	4.9	15.8

[a] d_{dis}: dispersed domain size. d: overall domain size.

Table 3. Calculated and Experimental Characteristic Distances for the PDMS*y*K−IP−B_2 Samples

	theo (Å)	NMR (Å)	ESCA (Å)	
y (KDa)	$\langle r^2\rangle^{1/2}$	$d - d_{dis}$	l	$l - \delta$
2.4	36	45	44	27
10	73	63	53	35
27	120	109	85	58

in good agreement with the $d - d_{dis}$ values, which are 63 and 109 (Table 3).

When the dimensionality of the dispersed phase is 2, in the case of PDMS2.4K−IP−B_2, the dispersed phase consists of cylinders and the two hard segments end capping the same soft segment, when the conformation of the soft segment leads to a small end-to-end distance, may be in the same cylinder. The average distance between the centers of two neighboring cylinders minus the cylinder diameter ($d - d_{dis}$) should be larger than the root-mean-square end-to-end distance of the soft segments, since, as explained above, a large portion of conformations of the soft segments that lead to small end-to-end distances are excluded from contributing to the calculation of the average distance between cylinders. The calculated $\langle r^2\rangle^{1/2}$ for PDMS (MW = 2.4 KDa is 36, which is indeed smaller than the $d - d_{dis}$ value, 45.

Thus when the dimensionality of the dispersed phase is 3, a characteristic dimension for the soft segments, $d - d_{dis}$, is proportional to the $\langle r^2\rangle^{1/2}$ of the soft segments. The proportionality in this case is very close to 1, which is not necessarily true in other cases. When the dimensionality of the dispersed phase is 2, $d - d_{dis}$ should decrease slower than $\langle r^2\rangle^{1/2}$ with decreasing molecular weight, and our data is in agreement with this prediction.

The same reasoning is also applicable when one compares the thickness of a PDMS-enriched surface layer with the $\langle r^2\rangle^{1/2}$ of the soft segments. ESCA data obtained on these materials indicated a PDMS-enriched top layer, which is followed by a hard-segment-enriched layer.[2] The concentration depth profile for the hard segments contains a maximum and is described by a four-parameter compound Gaussian distribution model. The distance between the surface and the maximum, l, can be assigned as the thickness of the PDMS-enriched layer; alternatively, $l - \delta$, where δ is the standard deviation of the Gaussian distribution, can be used. For PDMS (MW = 2.4, 10, and 27 KDa, l values are 44, 53, and 85, and $l - \delta$ values are 27, 35, and 58, respectively. The characteristic dimension for PDMS, l, or $l - \delta$, is proportional to the $\langle r^2\rangle^{1/2}$, when the dimensionality of the dispersed phase is 3, i.e., the volume fraction of the hard segments is <0.1. When the volume fraction of the hard segments is around 0.3, the dimensionality of the dispersed phase is 2, and the decrease in the characteristic dimension is slower than $\langle r^2\rangle^{1/2}$ with decreasing molecular weight. The ESCA data were obtained on annealed (120 °C, 15 min) samples, assuming $\lambda = 34$ Å.

How reliable are the NMR calculations? The relaxation measurements (which are also using some of the

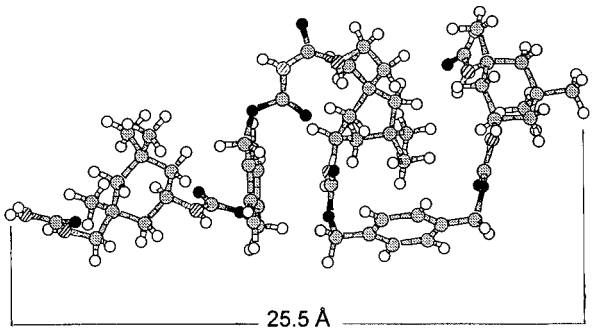

Figure 8. Minimized energy model of $B(CB)_2$ segment with the longest end-to-end distance: proton, open circle; carbon, dotted circle; nitrogen, lined circle; and oxygen, black circle.

same approximations) indicate that the dispersed phases of these samples should be between the distances obtained from $T_{1\rho}$(H) and T_1(H). The thermal analysis, which is normally sensitive to phase sizes down to 10 nm, does not "see" the dispersed phases, suggesting that the sizes of the hard phase in PDMS*y*K−IP−B_2 samples must be smaller than that. The ESCA measurements indicate that—at least within 25 Å—the top layer of a film may not contain any poly(urethane−urea) segments, and this seems to be well within the ranges found with NMR. However, in order to have a better idea about the real phase sizes, the actual spin diffusion coefficients and densities must be known.

Finally, a molecular simulation of the conformational arrangement of the hard phase ($B(CB)_x$) was performed for molecular formulas with $x = 1$ and 2 and compared with the experimental results. Several conformations of minimum energy can be found, and Figure 8 presents the model of PDMS*y*K−IP−B_2 with $x = 2$ which had the largest end-to-end distance, 25.5 Å. This result is in agreement with the NMR phase size. A sphere of some 5.5 nm diameter of the hard phase would contain several hard segments organized in an irregular fashion, and from the calculation it appears that there is plenty of space for this type of arrangement.

Conclusions

Solid-state NMR techniques were employed to show molecular dynamics differences and measure the domain size in PDMS*y*K−IP−B_2. More than one phase in PDMS*y*K−IP−B_2 is observed by spin−lattice relaxation parameters in the rotating frame. All motions in the PDMS*y*K−IP−B_2 samples increase with the increase of the molecular weight of PDMS. The domain sizes can be estimated using some approximations for the parameters such as spin diffusion coefficients, phase dimensionalities, and densities. The $T_{1\rho}$(H) and T_1(H) values can be used to estimate the domain size ranges. A more accurate domain size is obtained by spin diffusion NMR experiment by selecting for the mobile phase. The dispersed domain sizes of PDMS*y*K−IP−B_2 ($y = 2.4$, 10, and 27) do not change much with the increase of the molecular weight of PDMS. The overall domain sizes of PDMS*y*K−IP−B_2 ($y = 2.4$, 10, and 27) are about 10.1, 11.8, and 15.8 nm, respectively.

Acknowledgment. This work was supported in part by the Office of Naval Research. Funding for the NMR part comes from NSERC Canada in the form of a strategic grant. We thank ONR and NSERC Canada for support. A.N. thanks Canada Council for a Killam Research Fellowship.

References and Notes

(1) Ho, T.; Wynne, K. J.; Nissan, R. A. *Macromolecules* **1993**, *26*, 7029.
(2) Chen, X.; Gardella, J. A., Jr.; Ho, T.; Wynne, K. J. *Macromolecules* **1995**, *28*, 1635.
(3) Ho, T. Private communication.
(4) McBrierty, V. J. In *Comprehensive Polymer Science*; Allen, G., Ed.; Pergamon Press: Oxford, 1989; Vol. 1, p 397.
(5) Goldman, M.; Shen, L. *Phys. Rev.* **1966**, *144*, 321.
(6) Clauss, J.; Schmidt-Rohr, K.; Adam, A.; Boeffel, C.; Spiess, H. W. *Macromolecules* **1992**, *25*, 5208.
(7) Cai, W. Z.; Schmidt-Rohr, K.; Egger, E.; Gerharz, B.; Spiess, H. W. *Polymer* **1993**, *34*, 267.
(8) Spiegel, S.; Schmidt-Rohr, K.; Boeffel, C.; Spiess, H. W. *Polymer* **1993**, *34*, 4566.
(9) Clauss, J.; Schmidt-Rohr, K.; Spiess, H. W. *Acta. Polym.* **1993**, *44*, 1.
(10) Opella, S. J.; Frey, M. H. *J. Am. Chem. Soc.* **1979**, *101*, 5854.
(11) Connor, T. M. In *NMR Basic Principles and Progress*; Diehl, P., Fluck, E., Kosfeld, R., Eds.; Springer Verlag: New York, 1971; Vol. 4.
(12) Havens, J. R.; VanderHart, D. L. *Macromolecules* **1985**, *18*, 1663.
(13) Douglass, D. C.; Jones, G. P. *J. Chem. Phys.* **1966**, *45*, 956.
(14) Zumbulyadis, N. *Phys. Rev. B* **1986**, *33*, 6495.
(15) Clauss, J.; Schmidt-Rohr, K.; Spiess, H. W. *Macromolecules* **1992**, *25*, 3273.
(16) Cho, G.; Natansohn, A. *Can. J. Chem.* **1994**, *72*, 2255.
(17) Quirk, R. P.; Kinning, D. J.; Fetters, L. J. In *Comprehensive Polymer Science*; Allen, G., Ed.; Pergamon Press: Oxford, 1989; Vol. 7, p 1.
(18) Flory, P. J. *J. Am. Chem. Soc.* **1952**, *74*, 3364.

MA950777Q